Structural changes in loaded equine tendons can be monitored by a novel spectroscopic technique

Oksana Kostyuk, Helen L. Birch, Vivek Mudera and Robert A. Brown

University College London, Tissue Repair and Engineering Centre, Institute of Orthopaedics and Musculoskeletal Science, RNOH Campus, Brockley Hill, Stanmore HA7 4LP, UK

This study aimed to investigate the preferential collagen fibril alignment in unloaded and loaded tendons using elastic scattering spectroscopy. The device consisted of an optical probe, a pulsed light source (320–860 nm), a spectrometer and a PC. Two probes with either 2.75 mm or 300 μm source-detector separations were used to monitor deep and superficial layers, respectively. Equine superficial digital flexor tendons were subjected to *ex vivo* progressive tensional loading. Seven times more backscattered light was detected parallel rather than perpendicular to the tendon axis with the 2.75 mm separation probe in unloaded tendons. In contrast, using the 300 μm separation probe the plane of maximum backscatter (3-fold greater) was perpendicular to the tendon axis. There was no optical anisotropy in the cross-sectional plane of the tendon (i.e. the transversely cut tendon surface), with no structural anisotropy. During mechanical loading (9–14% strain) backscatter anisotropy increased 8.5- to 18.5-fold along the principal strain axis for 2.75 mm probe separation, but almost disappeared in the perpendicular plane (measured using the 300 μm probe separation). Optical (anisotropy) and mechanical (strain) measurements were highly correlated. We conclude that spatial anisotropy of backscattered light can be used for quantitative monitoring of collagen fibril alignment and tissue reorganization during loading, with the potential for minimally invasive real-time structural monitoring of fibrous tissues in normal, pathological or repairing tissues and in tissue engineering.

(Received 11 September 2003; accepted after revision 23 October 2003; first published online 24 October 2003)
Corresponding author O. Kostyuk: University College London, Tissue Repair and Engineering Centre, Institute of Orthopaedics and Musculoskeletal Science, RNOH Campus, Brockley Hill, Stanmore HA7 4LP, UK. Email: rehkrab@ucl.ac.uk

Tendons and ligaments are predominantly composed of the fibrous protein collagen and it is the highly ordered parallel packing of this structural component which provides great tensile strength. The striking level of collagen fibre organization and the anisotropic packing of these fibres are crucial to the mechanical functioning of the tendon. Furthermore, it is known, that changes in this structural organization due to ageing (Crevier-Denoix *et al.* 1998) or following tendon degeneration (Birch *et al.* 1998) or injury and repair (Williams *et al.* 1980) can result in loss of mechanical properties, failure and morbidity. This underlies many common sports or occupational injuries and may contribute to age-related arthritic disorders. At present there is no reliable technique to assess functional spatial fibre organization within living tendons (i.e. minimally invasive monitoring) at rest and under mechanical load. Such a technique would have a major impact in many branches of sports medicine, orthopaedics, paediatrics, reconstructive surgery and veterinary practice, allowing means of diagnosis and prognosis of disease or injury state and giving rapid quantitative outputs on recovery, therapeutic efficacy, etc.

Tendon has a hierarchical structure, with collagen molecules forming fibrils (50–500 nm), which in turn comprise a fascicle (50–300 μm), and fascicles align along the longitudinal axis of the tendon (Kastelic *et al.* 1978). Dense collagen fibril bundles are surrounded by thin connective tissue sheets, which delineate each fascicle. It is known that collagen fibrils within the fascicle have a waveform or crimp structure (Diamant *et al.* 1972) and this is straightened during mechanical loading of the tendon (Butler *et al.* 1978). Most commonly used techniques employed to study directional organization of soft tissues such as tendon are applicable for *in vitro* studies only, for example X-ray diffraction (Shah *et al.* 1991), and/or provide imaging information, such as polarized microscopy (Gathercole & Keller, 1991), optical coherent tomograpy (Hansen *et al.* 2002) and ultrasound (Ying

 DOI: 10.1113/jphysiol.2004.054809

et al. 2003). Such conventional tissue assessment relies on observation, which is qualitative and subjective, or it is destructive, retrospective and difficult to quantify over large volumes. NMR can provide quantitative information and it is a non-invasive technique (Fechete *et al.* 2003); however, it is very expensive. In contrast, a fibre-based optical monitoring technique may offer a cheap real-time minimally invasive alternative, which would make quantitative structural investigations widely available (e.g. general practice, physiotherapy, etc.).

Elastic scattering spectroscopy (ESS) is a novel cost-effective technique with a growing number of diagnostic applications in medicine (Bigio & Mourant, 1997). White light is delivered to the tissue surface by an optical fibre, where it can be reflected, scattered and/or absorbed. Backscattered light is collected by a detecting optical fibre and analysed by a spectrometer. Spectra of the backscattered light contain quantitative information about structure and composition of the tissue over significant volumes (mm^3) (Charvet *et al.* 2002). The depth of light penetration depends on the light wavelength, and the scattering and absorption properties of the tissue. The amount of backscattered light changes if the size of scattering particles or their relative refractive index changes. This phenomenon has been utilized, for instance, to diagnose malignant changes in human breast tissue (Ghosh *et al.* 2001) and colon (Zonios *et al.* 1999). The source–detector separation distance of the optical probe determines the tissue volume over which backscattered light is collected. When the detecting fibre is positioned very close to the illumination fibre, only backscatter from the superficial layers of the tissue can be detected (Canpolat & Mourant, 2001). However, increasing the distance between the illumination and detecting fibres allows light from the deeper regions of the tissue to reach the probe. Conventional understanding of reflectance spectroscopy indicates that narrow separation gives low volume/shallow sampling, relative to deeper sampling (with corresponding reduction in signal strength) for wider separations.

It has been shown previously that there is a significant anisotropy of backscattered light from tissues with some structural alignment, for instance muscle fibres in chicken breast tissue (Marquez *et al.* 1998) and collagen fibres in human skin (Nickel *et al.* 2000). This anisotropy arises from the fact that different amounts of light reach the detecting fibre if light travels along rather then across the structural components (fibres) of the tissue. We have successfully exploited this phenomenon in an *in vitro* experimental model to monitor the development of preferential fibre orientation in fibroblast-populated collagen gels subjected to uniaxial strain (Kostyuk & Brown, 2003). In this study we investigate the use of ESS to obtain quantitative information on fibre alignment in apparently healthy equine tendons. The equine superficial digital flexor tendon (SDFT) was used as its function is similar to that of the human Achilles' tendon and both these tendons show similar pathological changes prior to rupture. The SDFT is frequently injured in competition horses and therefore has been studied extensively. In addition, we explore the changes in spectra obtained from *in vitro* mechanically loaded tendons and discuss how this may relate to re-organization of fibres within the tendon during loading.

Methods

Tendon samples

The equine SDFT was used in this study. Tendons were collected from the forelimbs of seven horses destroyed humanely at a licensed abattoir operating under UK regulations, independently of this study for reasons other than tendon injury. Tendons were stored at –20°C and thawed at room temperature prior to measurements being taken.

Tendon loading/unloading regimes

Tendons were subjected to mechanical load by mounting in a vertical position in a hydraulic materials testing machine (Dartec) using cryoclamps to secure the ends with a gauge length of 10 cm and the mid-metacarpal region of the tendon centred between the clamps. After the tendon sample was positioned in the testing machine, a modest straightening force of 0.1 kN was applied and the elongation (strain) of the tendon was nominally considered to be zero at this load. Total load and strain (extension) were monitored, but not the cross-sectional area and hence stress was not controlled. Static loads (0.1–6 kN) were applied sequentially to the tendon, and then, following application of the maximum load, the loads were removed in a step-wise manner.

Optical set-up

The optical set-up as described earlier by Marenzana *et al.* (2002) consisted of an optical probe connected to a xenon light source and a spectrometer (Ocean Optics, FL, USA) and was controlled by a notebook PC. In this study two optical probes were used. A custom-made two-fibre probe contained a 400 μm diameter illumination fibre and a 200 μm diameter detection fibre, with 300 μm fibre

centre-to-centre distance, called the source–detector separation. Another probe with larger (2.75 mm) separation was assembled using the illumination fibre of the custom-made probe and a 200 μm diameter central fibre from a seven-fibre reflection probe (Knight Optical Technologies, Leatherhead, Surrey, UK) for detection. The axis between the illumination and detection fibres is termed here as the detection axis. The purpose of the two probe separations was to compare signals from very different sampling volumes/tissue depths (ideally suited to large tissues such as equine tendon).

Acquisition of the spectra

Tendon samples were illuminated with short pulses (~35 ms) of white light (320–860 nm) and spectra of the backscattered light were collected. A spectrum of the diffuse reflectance standard (Ocean Optics), recorded prior to each measurement session, was used as a reference to take into account spectral characteristics and overall intensity of the lamp. Measurements on unloaded tendons were made in the mid-metacarpal region with the tendon laid horizontally on a flat surface. The optical probe was positioned perpendicular to the tendon surface and the vertical position of the probe was ascertained using a manual rack pinion microscope stage (Fig. 1). Spectra were acquired with the probe touching the palmar aspect of the tendon (longitudinal set-up), using both probe separations. Further measurements were made by making a transverse cut through the tendon and placing the probe on to the cut surface with the light beam travelling parallel to the tendon longitudinal axis (transverse set-up). Spectra of the backscattered light were acquired for different angular positions (0, 45, 90, 270 and 315 deg) between the detection axis of the probe and the longitudinal axis of the tendon in the longitudinal set-up (since tendon has an axial symmetry, only a half-circle of rotation was performed in the longitudinal set-up). For this the tendon was rotated in the plane perpendicular to the optical probe. At the 0 deg position detected light travelled parallel with the tendon axis, and at the 90 and 270 deg positions the backscattered light passed in a perpendicular direction across the tendon fibres. For the transverse set-up of the tendons optical measurements were performed for the whole circle of rotation, at 45 deg intervals.

In the case of tendons under mechanical load, the optical probe was placed manually perpendicular to the palmar surface of the tendon in the mid-metacarpal region, and spectra with both probe separations were obtained. To obtain measurements at different angles between the detection axis and the longitudinal axis of the tendon the probe was rotated for a half-circle.

Three and seven tendon samples were investigated with 2.75 mm and 300 μm source–detector separations, respectively. Three or four spectra were collected from the same area of the tendon for each angular position of the probe and at each load applied.

Data analysis

Unprocessed optical spectra were transferred to the PC and analysed in EXCEL (Microsoft, USA). Spectra were normalized to the source light intensity by dividing by the number of incoming pulses of light. Normalized spectra were then transformed by dividing by the reference spectrum to account for a wavelength-dependent intensity of the light source; thus transformed spectra contained only information on the scattering/absorbing properties of the studied tissues. Spectra ($n = 3$–4) were averaged for each probe position. Backscattered light intensity at 500 nm was chosen as the chief parameter for investigation of the observed spatial anisotropy of light propagation, since the observed differences between the spectra were most pronounced at this wavelength (see Results). It is also important that at this wavelength contribution of haemoglobin absorption to spectra was negligible; moreover since 500 nm is an isosbestic wavelength, spectra were independent of any changes in haemoglobin oxygenation.

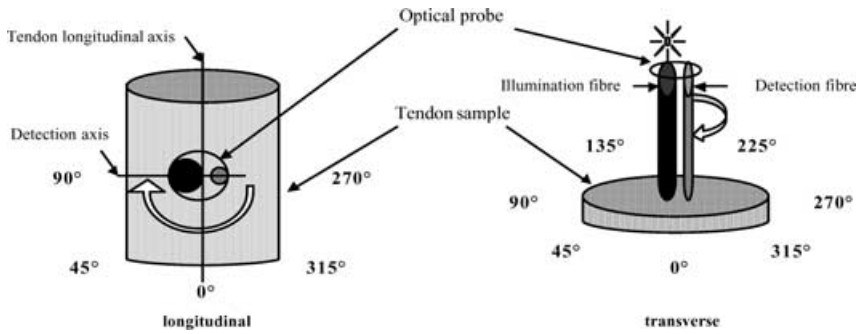

Figure 1. A schematic representation of the experimental set-up

To characterize the observed changes in the backscatter spatial anisotropy in the longitudinal set-up, an 'anisotropy factor', AF(500 nm), was calculated as the intensities ratio for angular positions with maximum and minimum intensities of backscatter at 500 nm:

AF(500 nm) = maximum backscatter intensity/minimum backscatter intensity

For the 2.75 mm separation probe, the maximum backscatter intensity occurred at the 0 deg position (light propagating parallel to the fibres) for all applied load regimes (except 0.1 kN), whereas the minimum was consistently at the 45 deg position. Therefore, AF_{II}(500 nm) was calculated as a ratio of backscatter intensities at 0 and 45 deg for the 2.75 mm separation probe. The plane of anisotropy was found to be perpendicular to the tendon axis for the 300 μm separation probe, so the respective anisotropy factor, AF(500 nm), was calculated as a ratio of backscatter intensities at the 90 and 0 deg positions.

Results

Unloaded tendons

The amount of backscattered light detected from unloaded tendons studied in the longitudinal set-up gradually increased with increasing wavelength for different positions of the probe with both probe separations (Fig. 2). For the 2.75 mm separation probe there was almost no backscattered light in the UV-blue region (350–420 nm) (Fig. 2*B*), whereas for the 300 μm separation probe measurable amounts of backscatter were registered even at these short wavelengths (Fig. 2*A*). This reflected a much higher overall intensity of backscattered light registered with the smaller probe separation (note a 100-fold difference in backscatter intensity detected with different separation probes). Spectra from transverse sections of the unloaded tendons were similar in shape to spectra from the longitudinal set-up for the 2.75 mm separation probe only (Fig. 3*B*). In contrast, spectra from the transverse sections acquired with the 300 μm separation probe differed in shape to those obtained in the longitudinal set-up. After a similar initial increase in backscatter intensity with wavelength up to approximately 520 nm, a significant decrease in intensity followed, so bell-shape spectra were observed (Fig. 3*A*). Characteristic haemoglobin absorption signatures were observed in both measurement set-ups and with both probe separations.

There was a substantial difference in intensity of backscattered light obtained at different positions of the probe (0, 45, 90, 270 and 315 deg) in the longitudinal set-up with both probe separations across all tendon specimens, i.e. there was a considerable spatial anisotropy of backscatter (compare spectra for 0 and 90 deg probe positions in Fig. 2). Observed differences in the backscatter intensities were most pronounced around 500 nm, so backscatter intensity at this wavelength was chosen for

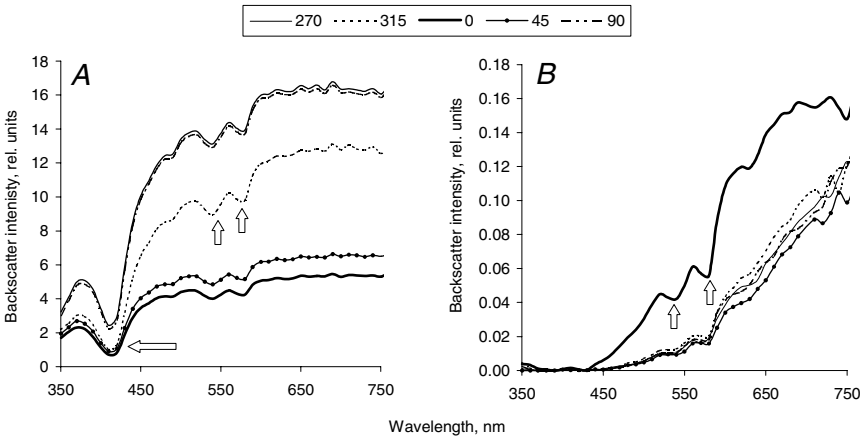

Figure 2. Spectra of backscattered light, acquired from the unloaded horse tendon (a representative sample) in a longitudinal set-up with 300 μm (*A*) and 2.75 mm (*B*) separation probes
The probe was placed perpendicular to the tendon surface, so light propagated perpendicularly to the tendon longitudinal axis. The tendon sample was rotated to achieve different angles between the tendon longitudinal and the probe detection axes. At the 0 deg position, the detection axis of the probe was parallel to the tendon axis, and at the 90 and 270 deg positions it was perpendicular to it. Each line represents a mean ($n = 3$) of spectra acquired from the adjacent areas of the tendon at the same position of the probe. Arrows indicate characteristic haemoglobin absorption signatures.

further analysis. In contrast, spectra obtained in the transverse set-up were much more uniform (Fig. 3).

A comparison between backscatter in the longitudinal and transverse set-ups at different positions of the probe is presented in the form of radial diagrams of the intensities of backscattered light at 500 nm (Fig. 4). In the longitudinal set-up at the 0 deg position the detection axis of the probe was parallel to the longitudinal axis of the tendon and it was perpendicular to it at 90 and 270 deg. There was 6.8 $\pm$ 2.3 (mean $\pm$ S.E.M., $n = 3$) times more backscattered light detected at 0 deg compared to 90 or 270 deg for the 2.75 mm separation probe (Fig. 4*B*). Thus, with the 2.75 mm separation probe, the maximum amount of backscatter was registered when light was travelling parallel to the longitudinal axis of the tendon (and the principal direction of tendon fibre alignment). Anisotropy in the orthogonal plane, perpendicular to the longitudinal axis of the tendon, was observed with the 300 μm separation probe: 3.1 $\pm$ 0.7 (mean $\pm$ S.E.M., $n = 7$) times more backscatter was detected at the 90 deg as opposed to the 0 deg positions of the probe (Fig. 4*A*). In sharp contrast, isotropic backscatter was observed in the transverse set-up using both probe separations. When sampling across the exposed cut surfaces of the collagen fibres, distribution of the fibrils was relatively isotropic around a 360 deg probe rotation.

Changes under mechanical loading

Structural changes are known to occur in the tendon with application of uniaxial tension and we next tested the idea that these might alter the spatial anisotropy of the backscattered light. The range of the applied load was from 0.1 to 6 kN and the maximum load varied from 2 to 6 kN depending on the size of the tendon. All tendon samples reached a similar strain of between 9.3 and 13.7% strain for the maximum load applied. The applied loads produced gradual progressive changes in the radial distribution of the backscatter intensity. These were clearly illustrated by the changed appearance of the radial diagrams of the backscatter intensity for all investigated tendon samples. Figure 5 shows a representative series of such diagrams obtained with the 2.75 mm separation probe from a typical tendon tested over the 0.1–6 kN range of load. There was an increase in the intensity of the backscattered light in the orthogonal direction (perpendicular to the tendon axis/fibres) in the starting position under the basal load (0.1 kN), giving two planes of anisotropy, along and across the collagen fibres (Fig. 5*A*). This was in contrast to the single plane of optical anisotropy parallel with the tendon axis/fibres at rest, i.e. before samples were mounted into the testing machine (compare the shapes of the diagrams in Fig. 5*A* with the diagram from the longitudinal set-up in

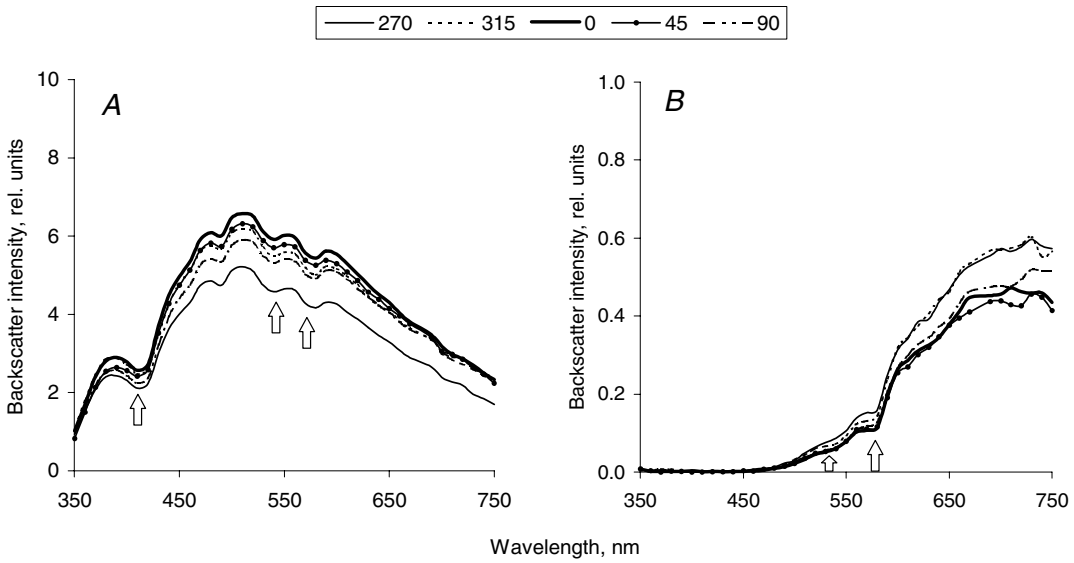

Figure 3. Spectra of backscattered light, acquired from the unloaded horse tendon (a representative sample) in a transverse set-up with 300 μm (*A*) and 2.75 mm (*B*) separation probes
The direction of light propagation coincided with the longitudinal axis of the tendon. The tendon sample was rotated to achieve different angular positions of the probe. Each line represents a mean ($n = 3$) of spectra acquired from the adjacent areas of the tendon at the same position of the probe. Arrows indicate characteristic haemoglobin absorption signatures.

Fig. 4*B*). As the load increased, the appearance of the radial diagrams reversed back to a bi-polar shape, with much higher intensities of backscattered light detected parallel to the principal strain and the tendon axis/fibres than in the perpendicular direction (Fig. 5*C*–*F*). These changes were consistent for all tendon specimens studied with the large probe separation. In contrast, radial diagrams of the backscatter intensities obtained with the small probe separation showed a gradual disappearance of the backscatter anisotropy in the perpendicular plane after an initial sharp 4.8 ± 1.8 (mean $\pm$ S.E.M., $n = 7$) times increase between the unloaded tendon and the tendon straightened with 0.1 kN (data not shown).

To characterize the observed changes in the backscatter spatial anisotropy in orthogonal planes during the tendon loading, anisotropy factors, $AF_{II}(500\ nm)$ and $AF(500\ nm)$ were calculated as the ratio between maximum and minimum intensities of backscatter, detected with 2.75 mm or 300 μm separation probes, respectively (see Methods). Load-dependent behaviour of both $AF_{II}(500$ nm) and AF(500 nm), obtained with different probe separations, and the corresponding strain is shown in Fig. 6 for a representative tendon sample. $AF_{II}(500$ nm) dramatically increased with increasing applied load in all investigated tendon samples. This increase was between 8.5- and 18.5-fold for individual tendons (maximal strains between 9.3 and 13.7%). In contrast, AF(500 nm) decreased between 1.9- and 6.5-fold for individual tendons in the same range of the applied load. There was a strong correlation between the optical ($AF_{II}(500$ nm) and AF(500 nm)) and mechanical (strain) parameters for all tendon samples tested. Correlation coefficients varied from +0.902 to +0.972 for $AF_{II}(500$ nm) and –0.892 to –0.978% for AF(500 nm).

In order to test if changes in anisotropy of backscattered light were reversible, we monitored both $AF_{II}(500$ nm) and AF(500 nm) while the applied load was decreased in a step-wise manner. Indeed, the $AF_{II}(500$ nm) recovered to its initial preloading value with some hysteresis effect (Fig. 7*B*) and AF(500 nm) was somewhat lower after the unloading compared to the at rest value (Fig. 7*A*).

Discussion

Light or electron microscopy (with image analysis) and X-ray diffraction methods are considered to provide a 'gold standard' analysis of matrix structure. However, current needs of clinical diagnostics and implant or tissue engineering monitoring make it imperative to find new cheap minimally invasive real-time analytical techniques to provide quantitative structural information. Clearly, such techniques must perform well against gold-standard

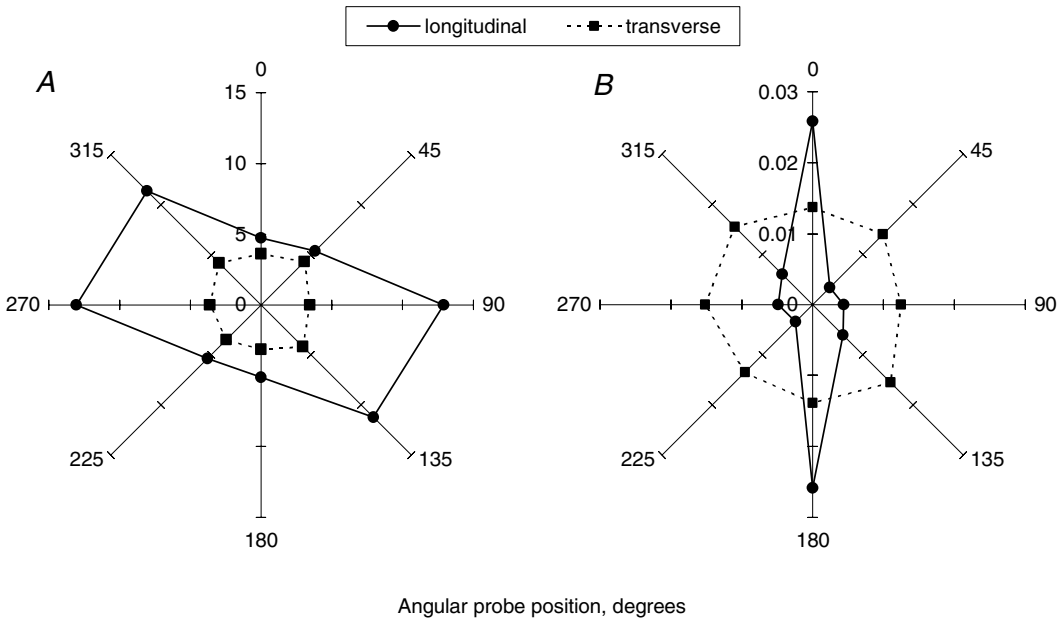

Figure 4. Radial diagrams of the intensity of backscattered light at 500 nm from unloaded tendons obtained in longitudinal and transverse measurement set-ups with 300 μm (*A*) and 2.75 mm (*B*) separation probes

Each data-point represents a mean of $n = 7$ and $n = 3$ tendon samples for 300-μm and 2.75-mm probe separations, respectively.

imaging techniques over significant volumes of tissue. Lack of such techniques is increasingly hindering progress not only in diagnostics, but critically, in development of new tissue engineered implants, therapeutic interventions particularly involved in sites of slow repair such as tendon, ligament, cartilage and nerve.

The results of this study suggest that ESS could play an important role in investigating normal dynamic *in situ* physiology. ESS interacts with the tissue via white light in the non-harmful range of wavelength (visible light) and at relatively low intensities, hence providing a non-harmful technique. The optical probe could be applied alongside current arthro- or endoscope procedures, making it minimally invasive. Furthermore, with the future development of computerized algorithms for data analysis, the technique could provide real-time structural information at low cost (prototype $\sim$ 5000).

To appreciate the results of this study, it is necessary to understand what microstructures in tendons are responsible for the backscatter of light. Smitt & Kumar, 1998), using a microoptical model of soft biological tissue, found that the diameters of scattering particles that contribute most to backscattering were in the order of half to a quarter of the wavelength applied. Based on this observation, we conclude that tendon structures responsible for the backscattered light at 500 nm in our study were 125–250 nm in diameter. This corresponds to the size of collagen fibrils in tendon fascicles, which is between 50 and 500 nm (Kastelic *et al.* 1978).

If ESS is to be used as a research and diagnostic tool it is important to know what depth or volume of tissue is examined. Tuchin (1997) stated that short-wave visible light penetrates typical biotissues up to 2.5 mm and at 0.6–1.5 μm wavelengths light reaches up to 10 mm. It was also estimated experimentally, using India ink injection, that a 1.9 mm diameter probe with source–detector separations ranging from 0.3 to 1.4 mm tested mouse skin up to a depth of 1 mm

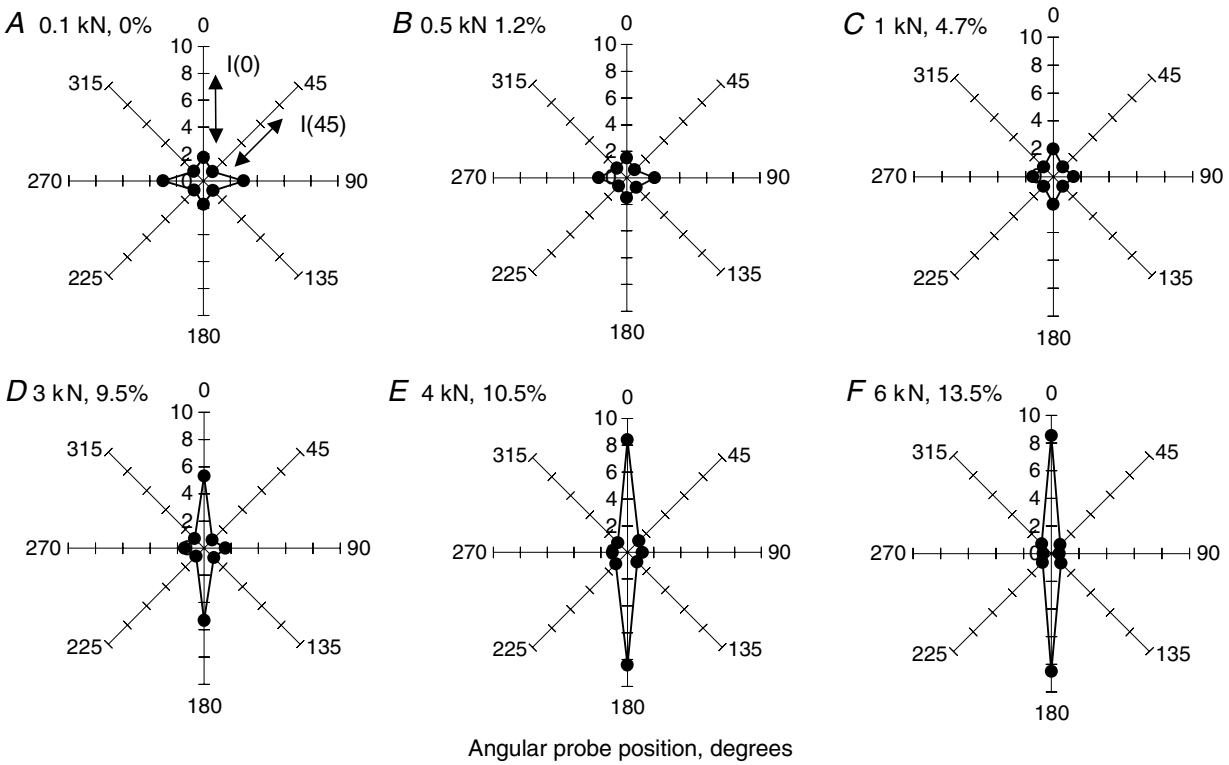

Figure 5. A series of radial diagrams of the intensity of backscattered light at 500 nm for a representative tendon subjected to the progressive uniaxial loading (load, strain)

A, 0.1 kN, 0%; *B,* 0.5 kN, 1.2% *C,* 1 kN, 4.7%; *D,* 3 kN, 9.5%; *E,* 4 kN, 10.5% *F,* 6 kN, 13.5%. Each data-point represents mean ($n = 3$) of backscatter intensities from the spectra taken from adjacent areas of the tendon at the same position of the probe. In each diagram light intensities at different angular positions were normalized to the respective light intensity at 45 deg, so direct comparison between different loads could be made. Anisotropy factor, AF_{II}(500 nm), was calculated as a ratio between backscatter intensities at 0° and 45° positions of the probe.

with a total tissue volume of about 1 mm^3 (Charvet *et al.* 2002). Marquez *et al.* (1998) calculated maximum penetration depths of 1.9 cm while studying chicken breast muscle with a linear fibre array probe with approximately 1.2 cm maximum separation. Since the tendon has less chromophores than skin and muscle (no melanin and much less haemoglobin), less light will be absorbed. We estimate therefore that in our experiments the 2.75 mm separation probe would register backscatter to a depth of 2–3 mm within the tendon. Based on the probe geometry, we assume significant backscatter could only be picked up from half of the illuminated tissue volume. This gives an estimated studied tissue volume of 16–54 mm^3 (half of a sphere with a diameter of 2–3 mm), which means that in our study the 2.75 mm separation probe was detecting backscattered light from the main load-bearing interior of the tendon. The 300 μm separation probe probably detected backscattered light not more than 300 μm ($\sim$0.06 mm^3), corresponding to a very superficial layer of the tendon. This is anatomically quite significant as the tendon structure at the surface is quite distinct and does not represent the structure of the interior load-bearing tendon areas. Tendon is surrounded by a layer of connective tissue known as epitenon, a fine, loose sheath, which extends deeper into the tendon between the tertiary bundles as the endotenon (Khan *et al.* 1999). This tissue has a thickness of up to 200 μm in the equine SDFT (H. Birch, unpublished data). Hence, the backscattered light detected using the 300 μm separation probe was mainly due to superficial epitenon.

To make predictions about the structural changes in tendon from ESS it is necessary to understand the basis for anisotropy of backscattered light. It has been shown experimentally that structurally anisotropic tissues such as skin (Nickel *et al.* 2000) and muscle (Marquez *et al.* 1998) produce backscatter anisotropy. A possible mechanism for 'light-guiding' by tissue fibres was suggested (Marquez *et al.* 1998). Moreover, Monte-Carlo simulations of partly orientated scatterers predicted the observed anisotropy (Nickel *et al.* 2000) and were used to work out a proportion of aligned fibres on a background of randomly orientated fibres.

We observed substantial anisotropy of light backscatter in unloaded tendons studied in the longitudinal set-up. To our knowledge, this is the first report of optical anisotropy in tendons observed with non-polarized light. Measurements made with the large probe separation produced anisotropic backscatter, which coincided with the longitudinal axis of the tendon. We conclude that the observed backscatter anisotropy was dependent on (and therefore a measure of) longitudinal collagen fibril alignment in the tendon interior (up to 3 mm deep) and the fact that backscattering was isotropic for the transverse set-up corroborates this conclusion.

Unexpectedly, two orthogonal planes of anisotropy were observed using different probe separations. In contrast to the 2.75 mm separation probe, the small separation probe produced anisotropy in a perpendicular plane to the long axis of the tendon, which was detected mainly from the tendon superficial layer (epitenon). Based on the

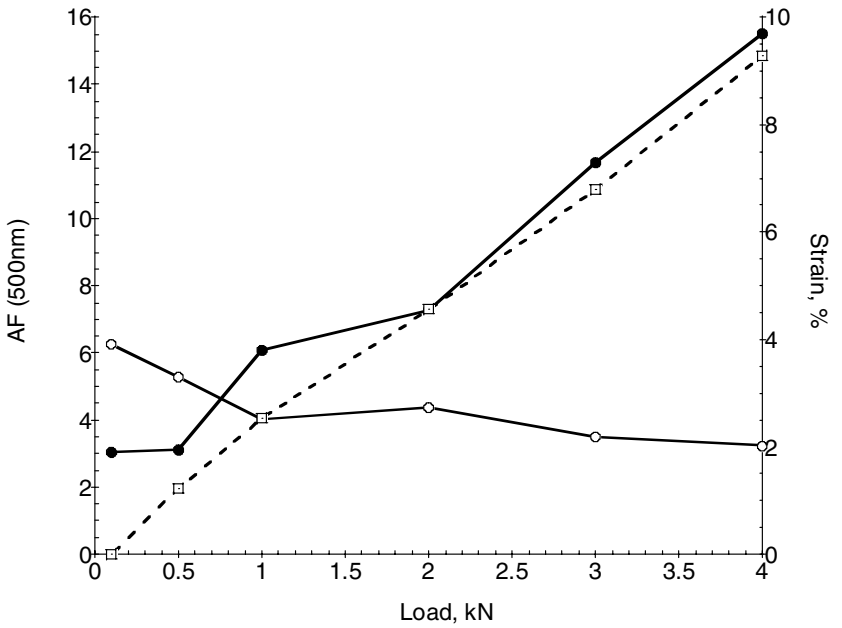

Figure 6. Anisotropy of backscattered light in perpendicular and parallel directions relative to the longitudinal axis of the tendon, and strain for a representative tendon sample as a function of applied load
AF (500 nm) —○—, $AF_{||}$(500 nm) —•—, strain - -□- -. Since tendons varied in size, different strains were achieved for the same loads, thus data for a representative tendon are presented. $AF_{||}$ (500 nm) and AF (500 nm) were anisotropy factors for the 275 μm and 300 μm probe separations, respectively.

direction of anisotropy observed with the small separation probe, we suggest that collagen fibrils in this layer, known to be randomly arranged (Johnston, 1985), align at least in part around the circumference of the tendon (i.e. perpendicularly to the longitudinal axis of the tendon).

The degree of anisotropy was larger for the 2.75 mm separation probe (parallel to the tendon axis) compared to the anisotropy measured with the 300 μm separation probe (in the perpendicular plane), with more than a 2-fold difference. This could be explained by the larger volume of the highly organized tissue probed with the 2.75 mm separation probe (since volumes of >10 mm^3 will include a number of tendon fascicles) compared to the low-volume sampling over much less organized superficial epitenon achieved with the smaller separation probe.

Applying mechanical loads to the tendon resulted in progressive and predictable structural changes within the tendon. As it is stretched fascicles and fibres in the tendon deep load-bearing interior align, collagen fibre crimp disappears (Butler *et al.* 1978), fibre diameter decreases and displacement of liquid occurs (Han *et al.* 2000). Changes in both relative refractive index of scattering structures (e.g. fibril packing, water loss and changes in fibril diameter) alter the backscatter signature, but their influence on anisotropy is uncertain. However, it can be envisaged that loss of crimp will increase optical anisotropy, as the collagen fibril alignment increases. This was seen as an 8.5- to 18.5-fold increase in backscatter anisotropy parallel to the tendon axis (2.75 mm separation probe) in progressively loaded tendons with the maximum strain varying between 9.3 and 13.7%. This finding agrees with the observed increased optical anisotropy in human skin related to the direction of stretching (Nickel *et al.* 2000). Apparently, structural changes in tendons responsible for the anisotropic backscatter were reversible since the observed anisotropy recovered its values during the tendon unloading. Strains measured *in vivo* for the same tendon produced values of up to 7.6% at the walk, 10.1% at the trot, and 16.6% at the gallop (Stephens *et al.* 1989); thus the strains tested in this study were within the physiological range. Therefore, we conclude that increased backscatter anisotropy reflects the increased alignment of tendon collagen fibrils and could be used as a reliable quantitative marker of its structural reorganization during physiological loading. The basal resting load of normal equine tendons *in vivo* is not known (but will be significant) and so some aspects at the (undetermined) lower end of loading (seen in these *ex vivo* specimens) will have little relevance to physiological conditions (though they are important). Studies are in progress to determine the *in situ* functional range of optical changes (X. Morgan, O. Kostyuk, V Mudera and R. A. Brown, in preparation).

It is known that tensile loading and deformation of the tendon core will also produce a relatively higher compression in the superficial collagen layer (epitenon).

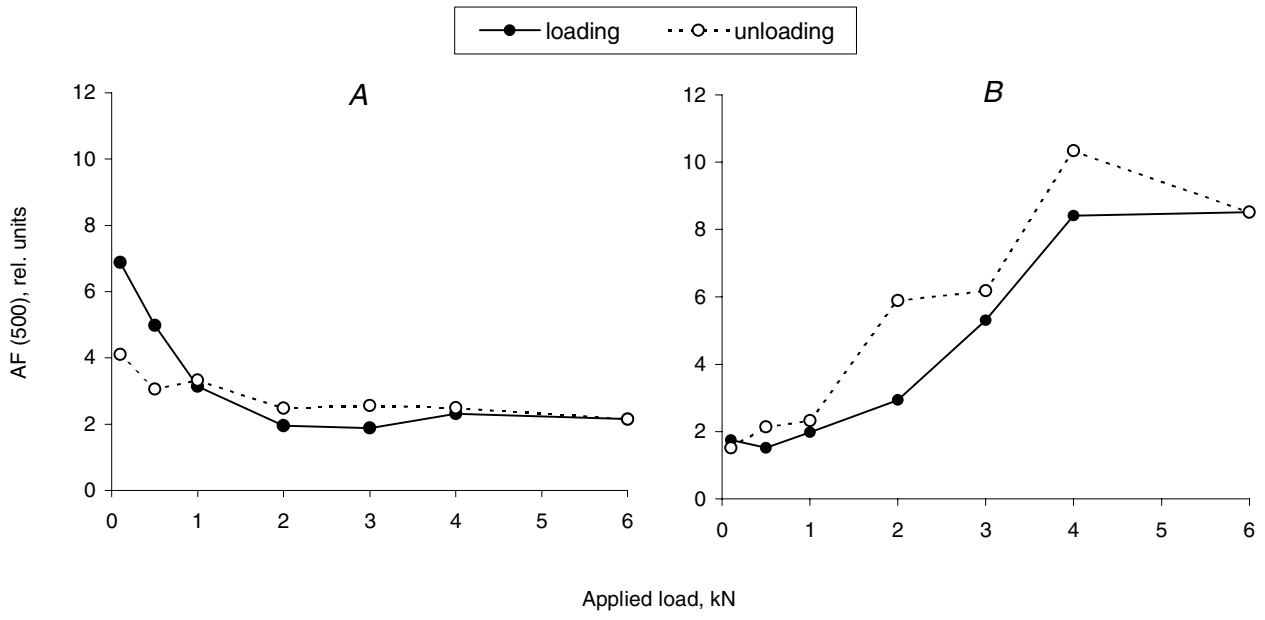

Figure 7. Anisotropy of backscattered light, $AF_{\perp}$(500 nm) (*A*) and AF_{II}(500 nm) (*B*), during loading and unloading of a representative tendon sample

Maximal strain of 13.4% was achieved in this tendon with the maximum of applied load, 6 kN. After unloading, residual extension of the tendon was equal to 5.4% of its length at the beginning of the load application.

This is likely to explain the pronounced backscatter anisotropy in the plane, perpendicular to the tendon axis, seen with the smaller separation probe. Compressive strain elements at interfaces will tend to realign fibres in the orthogonal plane to the main force, as the shape of the tendon cross-sectional area changes. Under tensile load the tendon cross-section geometry changes from a low aspect oval to a high aspect oval shape with increasing circumferential length. Indeed, an increase in the circumference from 42.5 to 52 mm (25%) was observed in tendons under 6 kN load. The greatest anisotropy of backscatter perpendicular to the tendon axis was at the start of loading (0.1 kN). This element was also apparent in the backscatter radial diagram obtained using the large separation probe at the start of the loading. In the present system, this geometric change may have been emphasized by additional flattening of the ends of the tendon sample by the cryoclamps. Progressive thinning of the epitenon under load would also mean that underlying large parallel collagen fibres will contribute more to the backscatter signature (even at small separation). This may explain the decrease in anisotropy in the perpendicular plane with the increasing load, as the contributions from fibres aligned in orthogonal planes would effectively compensate each other. The sensitivity of surface epitenon matrix to even a modest load and deformation of the tendon as a whole has important biomechanical implications. Optical anisotropy, then, provides novel insights into the very distinctive matrix and cytomechanical environment of the epitenon, which is likely to be functionally important.

The optical parameter, anisotropy, showed a close correlation with the mechanical parameter, strain. This suggests that the structure of the matrix changes with mechanical strain in a predictable manner. A high level of reproducibility and consistency between specimens was observed. This suggests that ESS is a reliable technique, which could be developed further to measure strain and structural changes in living tendons. ESS analysis using optical fibre signal collection is ideal for applications in diagnostics, treatment-monitoring and tissue engineering. Availability of ultrathin arthroscopes, 0.68 mm in diameter (Kondoh & Westesson, 1991), will make further development even more attractive. A wide variety of additional information is clearly available from load responsive anisotropic signatures. In this study we have identified the baseline fibril orientation changes associated with normal load deformation of healthy tendons. These included fibre hyperalignment (corresponding to the loss of crimp) and the apparently reactive, circumferential strain-related alignment in the epitenon. Future studies are needed to identify dynamic real-time *in vivo* changes during growth, repair and due to tendon degenerative changes.

References

Bigio IJ & Mourant JR (1997). Ultraviolet and visible spectroscopies for tissue diagnostics: fluorescence spectroscopy and elastic-scattering spectroscopy. *Phys Med Biol* **42**, 803–814.

Birch HL, Bailey AJ & Goodship AE (1998). Macroscopic 'degeneration' of equine superficial digital flexor tendon is accompanied by a change in extracellular matrix composition. *Equine Vet J* **30**, 534–539.

Butler DL, Grood ES, Noyes FR & Zernicke RF (1978). Biomechanics of ligaments and tendons. *Exerc Sport Sci Rev* **6**, 125–181.

Canpolat M & Mourant JR (2001). Particle size analysis of turbid media with a single optical fiber in contact with the medium to deliver and detect white light. *Appl Optics* **40**, 3792–3799.

Charvet I, Thueler P, Vermeulen B, Saint-Ghislain M, Biton C, Jacquet J, Bevilacqua F, Depeursinge C & Meda P (2002). A new optical method for the non-invasive detection of minimal tissue alterations. *Phys Med Biol* **47**, 2095–2108.

Crevier-Denoix N, Collobert C, Sanaa M, Bernard N, Joly C, Pourcelot P, Geiger D, Bortolussi C, Bousseau B & Denoix JM (1998). Mechanical correlations derived from segmental histologic study of the equine superficial digital flexor tendon, from foal to adult. *Am J Vet Res* **59**, 969–977.

Diamant J, Keller A, Baer E, Litt M & Arridge RG (1972). Collagen; ultrastructure and its relation to mechanical properties as a function of ageing. *Proc R Soc Lond B Biol Sci* **180**, 293–315.

Fechete R, Demco DE, Blümich B, Eliav U & Navon G (2003). Anisotropy of collagen fiber orientation in sheep tendon by ^{1}H double-quantum-filtered NMR signals. *J Magn Reson* **162**, 166–175.

Gathercole LJ & Keller A (1991). Crimp morphology in the fibre-forming collagens. *Matrix (Stuttgart, Germany)* **11**, 214–234.

Ghosh N, Mohanty SK, Majumder PK & Gupta PK (2001). Measurement of optical properties of normal and malignant human breast tissue. *Appl Optics* **40**, 176–184.

Han S, Gemmell SJ, Helmer KG, Grigg P, Wellen JW, Hoffman AH & Sotak CH (2000). Changes in ADC caused by tensile loading of rabbit Achilles tendon: evidence for water transport. *J Magn Reson* **144**, 217–227.

Hansen KA, Weiss JA & Barton JK (2002). Recruitment of tendon crimp with applied tensile strain. *J Biomed Eng* **124**, 72–77.

Johnston DE (1985). Tendons, skeletal muscles, and ligaments in health and disease. In *Textbook of Small Animal Orthopaedics*, ed. Newton, CD & Nunamaker, DM, pp. 65–76. JP Lippincott Co., The Washington Square Press, Philadelphia, USA.

Kastelic J, Galeski A & Baer E (1978). The multicomposite structure of tendon. *Connect Tissue Res* **6**, 11–23.

Khan KM, Cook JL, Bonar F, Harcourt P & Åstrom M (1999). Histopathology of common tendinopathies: Update and implications for clinical management. *Sports Med* **27**, 393–408.

Kondoh T & Westesson PL (1991). Ultrathin arthroscope for use in the lower compartment of the temporomandibular joint. *Oral Surg Oral Med Oral Pathol* **72**, 146–149.

Kostyuk O & Brown RA (2003). Orientation of collagen fibrils in tissue-engineered constructs can be determined using spatial anisotropy of diffused light reflectance. *Program and Abstract Booklet, 6th International Conf Cell Eng* (20–22 August, 2003), p. 21. Sydney, Australia.

Marenzana M, Pickard D, MacRobert AJ & Brown RA (2002). Optical measurement of three-dimentional collagen gel constructs by elastic scattering spectroscopy. *Tissue Eng* **8**, 409–418.

Marquez G, Wang LV, Lin SP, Schwartz JA & Thomsen SL (1998). Anisotropy in the absorption ans scattering spectra of chicken breast tissue. *Appl Optics-OT* **37**, 798–804.

Nickel S, Hermann M, Essenpreis M, Farrell TJ, Krämer U & Patterson MS (2000). Anisotropy of light propagation in human skin. *Phys Med Biol* **45**, 2873–2886.

Shah JS, La Monaca A, Bigi A & Roveri N (1991). X-ray diffraction and continuous small-angle scattering of turkey tendons with the improved area detector at Frascati. *Nucl Instrum Meth A* **A308**, 285–290.

Smitt JM & Kumar G (1998). Optical scattering properties of soft tissue: a discrete particle model. *Appl Optics* **37**, 2788–2797.

Stephens PR, Nunamaker DM & Butterweck DM (1989). Application of a Hall-effect transducer for measurement of tendon strains in horses. *Am J Vet Res* **50**, 1089–1095.

Tuchin VV (1997). Light scattering study of tissues. *Physics – Uspekhi Fizicheskih Nauk (Russian Acad Sci)* **40**, 495–515.

Williams IF, Heaton A & McCullagh KG (1980). Cell morphology and collagen types in equine tendon scar. *Res Vet Sci* **28**, 302–310.

Ying M, Yeung E, Li B, Li W, Lui M & Tsoi CW (2003). Sonographic evaluation of the size of Achilles' tendon: the effect of exercise and dominance of the ankle. *Ultrasound Med Biol* **29**, 637–642.

Zonios G, Perelman LT, Backman V, Manoharan R, Fitzmaurice M, Van Dam J & Feld MS (1999). Diffuse reflectance spectroscopy of human adenomatous colon polyps *in vivo*. *Appl Optics* **38**, 6628–6637.

Acknowledgements

This research was supported by the EPSRC (GR/R43594/01), European Union 'BITES' programme (QLK3-CT-1999-00559) and The Home of Rest for Horses (UK).